Substitutions in the aspartate transcarbamoylase domain of hamster CAD disrupt oligomeric structure

Yu Qiu and Jeffrey N. Davidson*

Department of Microbiology and Immunology, Albert B. Chandler Medical Center and Lucille P. Markey Cancer Center, University of Kentucky, Lexington, KY 40536-0084

Edited by George R. Stark, Cleveland Clinic Foundation, Cleveland, OH, and approved November 10, 1999 (received for review September 7, 1999)

Aspartate transcarbamoylase (ATCase; EC 2.1.3.2) is one of three enzymatic domains of CAD, a protein whose native structure is usually a hexamer of identical subunits. Alanine substitutions for the ATCase residues Asp-90 and Arg-269 were generated in a bicistronic vector that encodes a 6-histidine-tagged hamster CAD. Stably transfected mammalian cells expressing high levels of CAD were easily isolated and CAD purification was simplified over previous procedures. The substitutions reduce the ATCase V_{max} of the altered CADs by 11-fold and 46-fold, respectively, as well as affect the enzyme's affinity for aspartate. At 25 mM Mg^{2+}, these substitutions cause the oligomeric CAD to dissociate into monomers. Under the same dissociating conditions, incubating the altered CAD with the ATCase substrate carbamoyl phosphate or the bisubstrate analogue *N*-phosphonacetyl-L-aspartate unexpectedly leads to the reformation of hexamers. Incubation with the other ATCase substrate, aspartate, has no effect. These results demonstrate that the ATCase domain is central to hexamer formation in CAD and suggest that the ATCase reaction mechanism is ordered in the same manner as the *Escherichia coli* ATCase. Finally, the data indicate that the binding of carbamoyl phosphate induces conformational changes that enhance the interaction of CAD subunits.

Aspartate transcarbamoylase (ATCase; EC 2.1.3.2) catalyzes the formation of carbamoyl aspartate from carbamoyl phosphate and aspartate. In animals, the ATCase is covalently linked with two other enzymes catalyzing steps of *de novo* pyrimidine biosynthesis on a 240-kDa polypeptide called CAD—namely, carbamoyl-phosphate synthetase (CPSase; EC 6.3.5.5) and dihydroorotase (DHOase; EC 3.5.2.3) (1, 2). The ATCase domain is located at the C terminus of CAD. The native form of CAD is a complex of hexamers and trimers of identical subunits (1).

Escherichia coli ATCase is an independent monoenzymatic protein composed of two catalytic trimers held together through interactions with three regulatory dimers (3). CAD ATCase corresponds to the catalytic subunit of *E. coli* ATCase but is not allosterically regulated. The mammalian ATCase has 44% identity with the catalytic subunit of the *E. coli* enzyme (4). It has been predicted that they are structurally very similar (5, 6). X-ray crystallography (3) and site-directed mutagenesis studies (7) of *E. coli* ATCase have shown that specific residues form salt linkages between catalytic subunits, serving to hold the subunits together. This interaction is essential to the formation of the active site, which exists at the interface of catalytic subunits (3). Asp-90 and Arg-269 are such a pair of residues that interact at the interface of C1 and C2 subunits, respectively (7).

Building on the base of the *E. coli* ATCase structural data and the conservation of these residues in all known species (8), we wanted to examine the importance of these residues in the structural integrity and enzymatic function of hamster CAD. For simplicity, the *E. coli* numbering system is used such that Asp-90 and Arg-269 refer to hamster CAD residues Asp-2009 and Arg-2187, respectively. Alanine substitutions for these two residues were first performed using the hamster ATCase domain expressed in *E. coli* as a fusion protein with the *E. coli* maltose-binding protein (MBP) (9). The MBP-ATCase fusion proteins (with either a wild-type or altered ATCase) were purified to near homogeneity by amylose affinity chromatography. In nondenaturing gel electrophoresis, the wild-type enzyme migrated as a pentamer or hexamer, the Asp-90 → Ala mutant migrated as a trimer, and the Arg-269 → Ala mutant migrated as a dimer. Additionally, both mutants exhibited increased sensitivities to thermal and urea denaturation. These results indicated that the association between Asp-90 and Arg-269 is required for the proper quaternary structure and stability. The substitutions also led to dramatic effects on the kinetic properties of the enzymes and suggested that maintenance of a proper oligomeric structure is essential for normal enzymatic activity of hamster ATCase, consistent with the active site being at the interface of catalytic subunits.

Here, we sought to determine the significance of these residues in the context of the complete CAD. It was possible that the other enzymatic domains of CAD might compensate for the Asp-90 → Ala or Arg-269 → Ala substitution in the ATCase domain. In fact, the data presented here support this theory.

Previously, full-length hamster CAD had been expressed in both mammalian cells (10) and bacteria (11). However, obtaining large quantities of purified CAD from either source has proved difficult. Moreover, expression of a mammalian protein in a bacterial system may provide an incomplete picture. Certain posttranslational modifications such as phosphorylation (10) do not occur in bacterial cells. For a rigorous consideration, we sought to highly express Syrian hamster CAD in cultured Chinese hamster ovary (CHO) cells deficient in their own CAD to establish a natural source of the enzyme. Traditional mammalian expression systems previously used in our lab were not efficient. Usually, after transfection into a CAD-deficient CHO cell line, complementation for the CAD deficiency was observed for only 10% of the G418-resistant colonies. Furthermore, CAD expression in these transfectants was very low, at most 20–35% of the wild-type level. Even for the highest expressing colony, CAD was not detectable on a Coomassie blue-stained SDS/PAGE gel of crude cell extract. It should be noted that crude extracts from wild-type CHO cells also do not yield a visible CAD band.

Here, a bicistronic construct was developed as an efficient, high expression system for CAD in mammalian cells. The bicistronic vector (12) utilizes the internal ribosome entry site (IRES) of the encephalomyocarditis virus, allowing the translation of both CAD and neomycin phosphotransferase from a single mRNA in mammalian cells. Furthermore, use of a 6-histidine tag added at the N terminus of CAD allowed purification

This paper was submitted directly (Track II) to the PNAS office.

Abbreviations: ATCase, aspartate transcarbamoylase; CPSase, carbamoyl-phosphate synthetase; DHOase, dihydroorotase; CAD, CPSase–ATCase–DHOase polypeptide; MBP, maltose-binding protein; PALA, *N*-phosphonacetyl-L-aspartate.

*To whom reprint requests should be addressed. E-mail: jndavid@pop.uky.edu.

The publication costs of this article were defrayed in part by page charge payment. This article must therefore be hereby marked "*advertisement*" in accordance with 18 U.S.C. §1734 solely to indicate this fact.

of the full-length protein from cell extracts in a single chromatographic step.

The high expression and purification system described here helped us to gain insights into the Asp-90 → Ala and Arg-269 → Ala substitutions in the full-length CAD.

Materials and Methods

Construction. Plasmid DNA was purified by using Qiagen columns. PCR amplifications were carried out with *Pfu* DNA polymerase (Stratagene). Site-directed mutagenesis was performed with the QuikChange Site-Directed Mutagenesis Kit (Stratagene). Restriction digestion, ligation, DNA fragment purification, and transformation were carried out according to standard procedures (13).

Cells and Transfection. The wild-type Chinese hamster ovary cell line CHO-K1 was used as a positive control for measuring CAD expression.

G9C cells were derived from CHO-K1 cells and maintained in Ham's F-12 medium containing 3 μM uridine and 10% fetal bovine serum.

Constructs were stably transfected into G9C cells by the calcium phosphate method (13). Transfectants were selected and maintained on Dulbecco's modified Eagle's medium (DMEM) (GIBCO) with 10% fetal bovine serum, 1 mg/ml G418 (Geneticin, GIBCO), and 3 μM uridine.

Protein Purification. Crude extract was prepared from 2×10^7 cells by sonication and centrifugation in 20 mM Tris·HCl, pH 7.9/0.5 M NaCl/5 mM imidazole/25 mM $MgCl_2$. Supernatant was loaded on a 1-ml Ni^{2+} column (Novagen) equilibrated with the same buffer. The column was then washed with 20 mM Tris·HCl, pH 7.9/0.5 M NaCl, with increasing concentrations of imidazole: 5 mM, 60 mM, and 100 mM. The 6-histidine-tagged CAD protein was eluted with 1 M imidazole in the buffer above. After elution, enzyme solution was immediately brought to 30% (vol/vol) DMSO, 5% (wt/vol) glycerol, and 1 mM DTT, then used freshly or stored at −70°C.

Concentrations of protein were determined by the method of Bradford (14), with the Bio-Rad protein assay dye.

Enzyme Assays. The assay for ATCase follows the conversion of [^{14}C]aspartate (Sigma) to carbamoyl[^{14}C]aspartate (9, 15). CPSase activity was measured by the incorporation of [^{14}C]bicarbonate (New England Nuclear) into [^{14}C]carbamoyl phosphate (16, 17) at 37°C. DHOase activity was assayed in the forward reaction by the conversion of [^{14}C]carbamoylaspartate (Moravek Biochemicals, Brea, CA) to dihydro[^{14}C]orotate at pH 6.0 (18).

The ATCase kinetic analysis for aspartate was performed with a radiometric procedure (19) that measures the conversion of [^{14}C]carbamoyl phosphate to [^{14}C]carbamoylaspartate. The reaction mixture contained 50 mM Hepes (pH 8.5), 2.5 mM [^{14}C]carbamoyl phosphate (0.125 μCi; 1 μCi = 37 kBq) (American Radiolabeled Chemicals, St. Louis), and 0.3–1.7 μg of the wild-type or altered CAD. Aspartate concentrations varied from 0 to 20 mM. After incubation at 37°C for 30 min, the reaction was quenched by 20% trichloroacetic acid, which converts the unincorporated carbamoyl phosphate to CO_2. Reaction mixtures were transferred to scintillation vials and were gently dried overnight at 70°C. The dried samples were resuspended in 100 μl of deionized H_2O, and 4 ml of scintillation solution was added before counting.

Glycerol Gradient Ultracentrifugation. Cells (1×10^7) were suspended in 500 μl of sonication buffer containing 50 mM Hepes (pH 7.4), 1 mM DTT, 25 mM $MgCl_2$, 25 mM KCl, 4 mM glutamine, 30% (vol/vol) DMSO, and 5% (wt/vol) glycerol. After sonication and addition of 20 mM $MgCl_2$, the supernatant was clarified by centrifugation at 18,000 × *g* at 4°C for 10 min.

The standard glycerol gradient contained 50 mM Hepes (pH 7.4), 1 mM DTT, 25 mM $MgCl_2$, 25 mM KCl, 4 mM glutamine, 30% (vol/vol) DMSO, and 8–20% (wt/vol) glycerol. A 0.5-ml cushion of 30% glycerol was added to the centrifuge tube before forming the gradient. Clarified supernatant (0.5 ml) was layered on top of the linear gradients. After centrifugation for 24 hr at 4°C with a speed producing 194,000 × *g* in a Sorvall RC70, the bottom of the tube was punctured and 8 drops were collected for each fraction. A DHOase assay of each fraction was used to determine the position of the wild-type and altered CAD.

For analysis with *N*-phosphonacetyl-L-aspartate (PALA), 0.5 ml of clarified supernatant was brought to a final concentration of 10 μM PALA and incubated with slow shaking at 4°C for 1 hr before being layered on top of the gradient. For analysis with both ATCase substrates, clarified supernatant (0.5 ml) was brought to 16 mM aspartate and 2.5 mM carbamoyl phosphate and slowly shaken at 4°C for 1 hr before layering on top of a gradient containing 16 mM aspartate and 2.5 mM carbamoyl phosphate. For analysis with individual ATCase substrates, clarified supernatant was mixed with either 16 mM aspartate or 2.5 mM carbamoyl phosphate and was slowly shaken at 4°C for 1 hr before loading onto a gradient that either had 16 mM aspartate and no carbamoyl phosphate or 2.5 mM carbamoyl phosphate and no aspartate.

Results

Construction of Plasmids. pCIN-CAD: A 6.7-kb *Eco*RI/*Bam*HI fragment of hamster CAD cDNA was subcloned into the pCIN4 bicistronic vector (12). The hamster CAD cDNA is located downstream of the cytomegalovirus (CMV) promoter in the first cistron and upstream of the neomycin-resistance gene located in the second cistron.

pCIN-His-CAD: A PCR product encoding a 6-histidine tag and a spacer region from pPROEX-1 (GIBCO) was engineered into pCIN-CAD at the sequence encoding the N terminus of hamster CAD. The resulting constructs were verified by DNA sequencing. The additional N-terminal sequence of the 6-histidine tag without protease cleavage site is MGHHHHHHDYD-N<u>MAALV</u>. . . (normal CAD N-terminal sequence underlined). The product of this gene was called CAD-wt.

Site-directed mutagenesis was performed on the *Not*I/*Bam*HI fragment of CAD cDNA that had been subcloned into pBluescript. The mutagenic primers for creating Asp-90 → Ala were 5′-GAATCCCTTGCCG<u>C</u>CTCTGTGCAGACCATG-3′ (mutation underlined) and a primer corresponding to the complementary strand. The mutagenic primers for creating Arg-269 → Ala were 5′-GCATCCGATGCCC<u>GC</u>AGTCAATGAGATAAG-3′ and a primer corresponding to the complementary strand. The mutations were confirmed by DNA sequencing.

The mutated CAD cDNA fragments were then subcloned into the *Not*I/*Bam*HI sites of pCIN-His-CAD. The recombinant constructs were again confirmed by DNA sequencing. The construct-encoded proteins were named CAD-D90A and CAD-R269A.

High Expression of Wild-Type and Altered CADs in Mammalian Cells. G9C cells have essentially no CAD protein (i.e., about 0.1% the ATCase activity of wild-type CHO-K1 cells), are unable to grow in medium lacking uridine, and have an undetectable reversion frequency (<1 in 10^{-8}) (D. Patterson, personal communication). After transfection of G9C with pCIN-CAD or pCIN-His-CAD, virtually all of the isolated G418-resistant colonies grew in uridine-deficient medium. This complementation suggests that significant levels of CAD are expressed in the stably transfected cells.

The vector pCIN-CAD was used to determine the efficiency

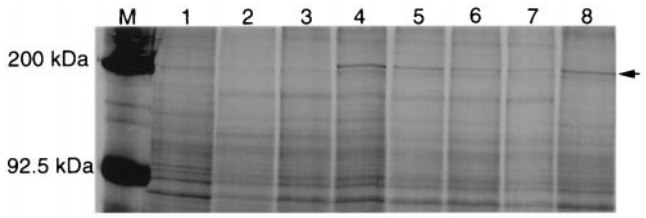

Fig. 1. SDS/PAGE screen for high expressing cell line. The cellular protein from each well of 96-well tissue culture plates was subjected to SDS/PAGE and stained with Coomassie blue. Lane M contains molecular mass markers. Lane 1 is the untransfected G9C cells. Lanes 2–11 are different clones of transfectants. The arrow indicates the band corresponding to CAD, which is observed only in lanes 4–8.

of generating stable transfectants expressing high levels of CAD protein. Transfected G9C colonies that grew on G418 were cultured in parallel on medium containing uridine, as a control, and on medium containing various concentrations of PALA (20), a transition-state analogue that inhibits ATCase (21, 22). The typical G418-resistant colony grew on 5 μM PALA, a concentration that corresponds to the LD_{50} for CHO-K1 cells. Some colonies even grew on 1 mM PALA. These results indicated that high level expression of the transgene in the pCIN bicistronic vector was easy to obtain.

A simple strategy was developed to identify clones that expressed high levels of wild-type or altered CADs. Clones of transfected G9C cells were cultured in parallel in two 96-well culture plates with media containing G418 and uridine. Total cellular protein from a single well of confluent cells was loaded on an SDS/polyacrylamide gel. Typically, half the clones produced a CAD band when gels were stained with Coomassie blue (Fig. 1), a feature not seen with total cellular protein from CHO-K1 or untransfected G9C cells. Those clones with the darkest CAD bands were cultured for obtaining cell-free extracts. The extracts were assayed for DHOase activity, and the activities observed were consistent with the density of the CAD band seen on gels. The single best transfectant of each type, CAD-wt, CAD-D90A, and CAD-R269A, was then used for the remainder of the experiments described.

Affinity Purification of Hamster CAD from the High-Expressing Mammalian Cells. After a single step of affinity chromatography, hamster CAD with a 6-histidine tag from transfectants of pCIN-His-CAD was affinity purified to greater than 95% homogeneity (Fig. 2). The affinity-purified CAD had the expected molecular mass of 240 kDa. Earlier procedures (1) for purifying CAD from cells amplified for an endogenous CAD gene generated an extra 190-kDa proteolytic fragment. The absence of significant bands of less than 240 kDa indicates that the 6-histidine-tagged CAD is not significantly cleaved by endogenous proteases.

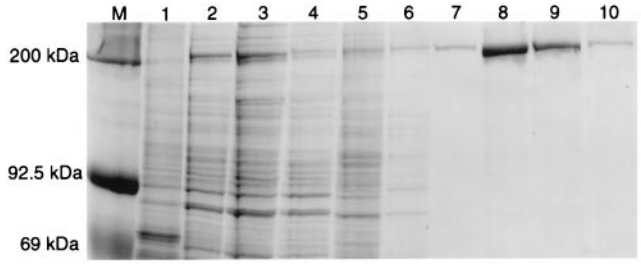

Fig. 2. CAD purification. Lanes 1 and 2 are cell-free extracts from an untransfected and CAD-wt-expressing cell lines, respectively. Extract from a CAD-wt-expressing cell line was then purified by Ni^{2+} affinity chromatography. Lane 3 is the flow-through. Lanes 4–6 are the washing steps with increasing concentrations of imidazole: 5 mM, 60 mM, and 100 mM. Lanes 7–10 are eluting fractions with 1 M imidazole. The SDS/PAGE gel was stained by Coomassie blue.

Table 1. Enzymatic activities of His-tag-purified enzymes

Enzyme	Specific activity, μmol/hr per mg			Ratio
	CPSase	ATCase	DHOase	
CAD-wt	1.4 ± 0.01	86.4 ± 4.8	47.4 ± 1.8	1:60:32
CAD-D90A	1.3 ± 0.03	12.5 ± 0.1	31.7 ± 1.4	1:10:25
CAD-R269A	1.2 ± 0.02	2.6 ± 0.4	29.4 ± 0.9	1:2:25

Enzymatic Activities of the Wild-Type and Altered CADs. To determine the catalytic activities of the recombinant CAD, the relative CPSase, ATCase, and DHOase activities were measured with the 6-histidine-tag-purified CAD enzymes. The ratios CPSase:ATCase:DHOase are shown in Table 1. The ratio of CAD-wt (1:60:32) is close to the previously published ratio for recombinant CAD (1:52:26) (23) partially purified from mammalian cells but without the 6-histidine tag. This result indicates that the 6-histidine tag at the N terminus of CAD does not interfere with any of the three catalytic activities. Our ratios are different from those reported by two groups, 1:38:11 (11) and 1:48:7 (1), probably because of differences in substrate concentrations and assay methods used.

Compared with the enzymatic ratio of the wild-type CAD, only the ATCase levels are significantly affected in the two substitutions, CAD-D90A and CAD-R269A (Table 1). These results indicated that the single substitutions in the ATCase domain reduce only the ATCase activity and do not appear to have any major effect that extends to the CPSase or DHOase activity.

Kinetic Analysis of ATCase in CAD. The aspartate saturation curves from the purified CAD-wt and the altered CADs are shown in Fig. 3. The substrate concentration giving 50% of V_{max}, $[S]_{0.5}$, of the 6-histidine-tagged CAD-wt is similar to that obtained from partially purified hamster CAD (9). As with MBP-ATCase, substrate inhibition was observed with CAD-wt, but absent in both CAD-D90A and CAD-R269A. A similar loss of substrate inhibition was also reported in the R269A substitution of the *E. coli* ATCase (7).

The catalytic properties of ATCase in CAD are affected by the replacements of Asp-90 and Arg-269 with alanine (Table 2). The V_{max} of CAD-D90A is 9% that of CAD-wt, while the corresponding value for CAD-R269A is 2%. The affinity for aspartate in CAD-D90A and CAD-R269A was decreased 5.5-fold and

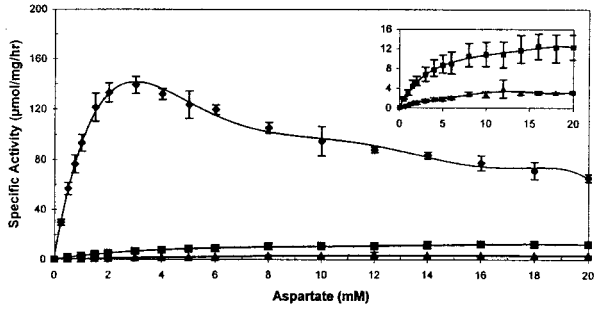

Fig. 3. Aspartate kinetic analysis of CAD ATCase. The assays were performed on purified CAD-wt (◆), CAD-D90A (■), and CAD-R269A (▲) in the absence of magnesium. Each point represents the mean ± SD from triplicate determinations. The details of the altered CADs are shown in the *Inset*.

Table 2. Kinetic parameters of ATCase in CAD

Enzyme	V_{max}, μmol/hr per mg	$[S]_{0.5}^{Asp}$, mM
CAD-wt	139 ± 6.7	0.65
CAD-D90A	12.5 ± 2.6	3.6
CAD-R269A	3 ± 0.3	7.3

Because of substrate inhibition, the maximal observed specific activity was defined as the V_{max}.

11-fold, respectively. Compared with the data from MBP-ATCase (9), in which the affinity for aspartate of MBP-D90A and MBP-R269A was reduced 540-fold and 826-fold, respectively, the influences of the substitutions on the $[S]_{0.5}$ for aspartate were much less significant in the context of the full-length CAD. One explanation for these data is that the additional domains of CAD in some way compensate for the loss of a single salt linkage between the C1 and C2 subunits of the ATCase in CAD. Still, the R269A substitution was most affected in both systems. Although $[S]_{0.5}$ values for carbamoyl phosphate were determined, they are not shown because, as described below, this substrate appears to affect the multimeric structure of the altered CADs.

Multimeric Structure. To investigate whether the ATCase substitutions disrupt the oligomeric structure of CAD, glycerol gradient centrifugation was used to estimate protein size. To reduce the likelihood of degradation or conformational change during a purification procedure, freshly prepared cell-free extracts were used directly to initiate the centrifugation. Afterward, the location of CAD within the gradients was determined by DHOase assay, as this activity is unaffected by the substitutions under study. As expected, CAD-wt migrated as a hexamer of 240-kDa subunits as reported previously (1). In contrast, the substitutions, CAD-D90A and CAD-R269A, when compared with the molecular weight standard, migrated as monomers (Fig. 4). To investigate the possibility that the observed changes in migration were because of proteolysis, an identical glycerol gradient ultracentrifugation was carried out and followed by individual assays for CPSase, DHOase, and ATCase on all fractions. The results (Fig. 6, shown in the supplementary material at www.pnas.org) indicated that all three enzymes comigrated as a multifunctional protein as expected with no evidence of proteolysis. Further proof that the altered CADs were full-length was gathered by SDS/PAGE. Protein from the peak fractions gave a band at 240 kDa.

The complete dissociation of the altered CADs to monomers was unexpected because previous studies (24, 25) have shown that the active sites of *E. coli* ATCase are formed at the interface

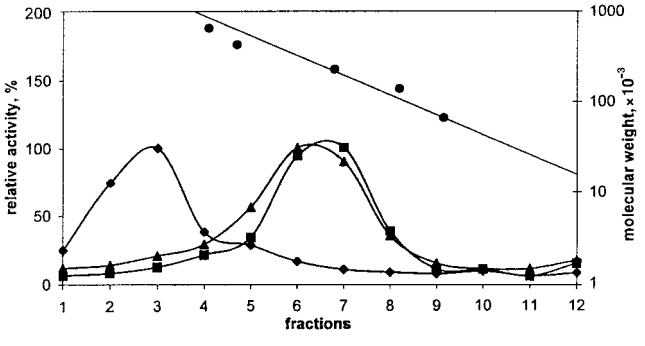

Fig. 4. Sedimentation of glycerol gradient in the absence of effectors. Wild-type CAD (◆), CAD-D90A (■), and CAD-R269A (▲) were sedimented on 8–20% glycerol gradients with 25 mM $MgCl_2$. The molecular weight standard (●) was run in parallel.

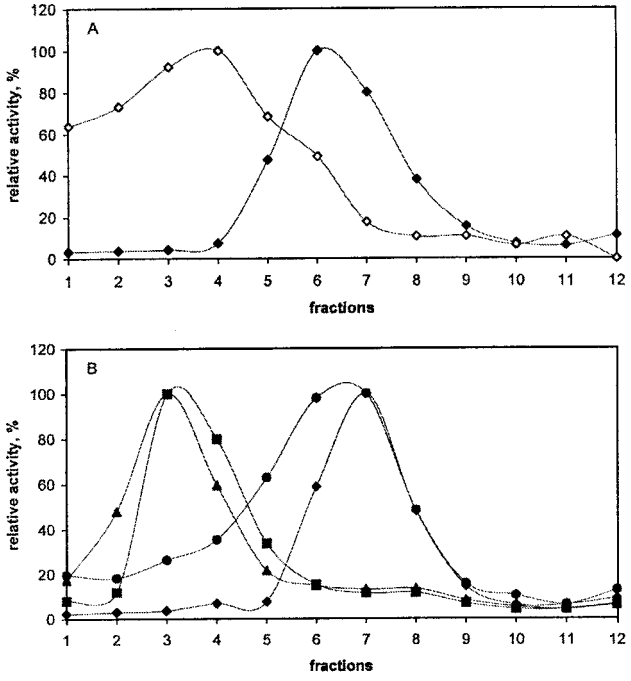

Fig. 5. Influence of different effectors to CAD-R269A sedimentation. (*A*) CAD-R269A sedimented through 4 mM $MgCl_2$ (◇) or 25 mM $MgCl_2$ (◆). (*B*) CAD-R269A incubated in the presence of 10 μM PALA (■) or in the absence of PALA (◆) before sedimentation and CAD-R269A incubated and sedimented with 1.6 mM aspartate (●) or 2.5 mM carbamoyl phosphate (▲). Mg^{2+} was present at 25 mM in all of the experiments shown in *B*.

of catalytic subunits. Given the significant ATCase activity of the altered CADs (Tables 1 and 2), it seemed unlikely that the protein was truly monomeric. Therefore, other factors were thought to contribute to oligomeric association/dissociation in the altered CADs. Of the several components of the glycerol gradient, only magnesium concentration appeared to affect the association/dissociation of CAD-R269A. In gradients containing a low concentration of magnesium (4 mM), CAD-R269A ran as a mixture of monomers, dimers, and higher oligomers, mostly higher oligomers (Fig. 5*A*). In contrast, the monomeric form was observed in gradients containing 25 mM $MgCl_2$. This result suggested that the ATCase substitutions weakened the oligomeric structures of CAD, allowing higher concentrations of magnesium to cause dissociation of oligomeric CAD to monomers. Magnesium concentration had no influence on the wild-type CAD. To determine whether Mg^{2+} concentration had some degree of specificity in oligomerization (i.e., C1–C2 interface interactions were strengthened with low Mg^{2+} and weakened with high Mg^{2+}), ATCase assays were performed in buffer containing either 25 mM or 4 mM magnesium. CAD-R269A was 2-fold less active in 25 mM $MgCl_2$, whereas there was no difference between high and low concentration of magnesium for the wild-type (data not shown). The association/dissociation effects of magnesium on CAD oligomerization proved reversible. When CAD-R269A protein was in 25 mM Mg^{2+} and loaded on a gradient with 4 mM Mg^{2+}, association was observed. When the reverse experiment was performed, dissociation to monomers occurred.

Magnesium concentration cannot fully account for oligomerization of the altered CADs. Under dissociating conditions of 25 mM $MgCl_2$, the CAD-R269A still had ATCase activity, albeit much reduced from CAD-wt levels. If a C1–C2 interaction is essential to ATCase activity, then the CAD-R269A protein must not be a monomer in the presence of substrates. The ATCase

substrates, aspartate and carbamoyl phosphate, were not present in the glycerol gradients, but were present when assaying gradient fractions for ATCase activity.

Perhaps the ATCase substrates or products facilitated oligomerization. To test this hypothesis, the transition state analogue, PALA, was incubated at 10 μM with CAD-R269A before loading on the glycerol gradient. After PALA preincubation, the CAD-R269A migrated as a hexamer just like CAD-wt rather than as a monomer (Fig. 5*B*). The same result was seen for CAD-D90A preincubated with PALA (data not shown). This result indicated that PALA could compensate for the loss of the Asp-90–Arg-269 pairing. Similar results were obtained from glycerol gradients containing both 16 mM aspartate and 2.5 mM carbamoyl phosphate where the sample protein was incubated with these substrates before centrifugation (data not shown).

E. coli ATCase is known to follow an ordered reaction, first binding carbamoyl phosphate, then binding aspartate. Therefore, to test whether a single substrate would allow oligomerization of CAD-R269A, saturating carbamoyl phosphate (2.5 mM) or aspartate (16 mM) was preincubated with cell extract from CAD-R269A-producing cells. Then the protein was loaded onto a glycerol gradient containing only that substrate. Preincubation with carbamoyl phosphate led to the same hexameric form seen when protein was treated with either PALA or both substrates together. In contrast, CAD-R269A remained monomeric when incubated with aspartate alone (Fig. 5*B*).

Discussion

In 1976, a PALA-resistant cell line overexpressing hamster CAD was created by Stark and his colleagues (22). CAD could be purified from these overproducing cells through a multistep purification procedure (1). Since then, the catalytic characteristics (19) and oligomeric structure (1, 26) of the wild-type CAD have been well studied. However, the allosteric regulation of the CPSase, metabolic channeling of intermediates, and the interactions between domains continue to be active areas of research. Because of the extremely large size of CAD, crystallographic data are not yet available, and site-directed mutagenesis remains the best approach to study the structure and function of hamster CAD. The PALA-resistant CAD-overexpressing cell line cannot be combined with site-directed mutagenesis. The standard purification procedure also produces a proteolytic byproduct (1). The system described here has overcome these two problems. We have also made further improvements on this system by replacing the downstream neomycin-resistance gene with the dihydrofolate reductase gene. Now, transfectants can be directly selected on high concentrations of methotrexate or selected by rounds of increasing concentrations of methotrexate. Levels of CAD expression up to 160 times that of CHO-K1 cells have been achieved (Y.Q., J. Ramsey, and J.N.D., unpublished data).

The 6-histidine tag is another advantage of this system. It allows the hamster CAD to be affinity purified to near homogeneity in one step. Purification takes less than 2 hr and is shorter than any previously published procedures for CAD. This rapid purification is helpful for maintaining enzymatic activity and may be responsible for preventing proteolytic degradation.

The oligomeric sizes of hamster CAD were described by Coleman *et al.* (1) as a mixture of mostly hexamers, trimers, and other oligomeric forms. This finding has been confirmed by other groups (11, 26, 27). Carrey (27) has proposed a CAD structure in which ATCase forms a trimer and DHOase forms a dimer, bringing together two CAD trimers. The CAD-D90A and CAD-R269A substitutions described here eliminated the pair of salt linkages formed between them, and conditions of high Mg^{2+} concentration disrupted any oligomerization of CAD. These results indicate that the CAD ATCase has a central role in all oligomer formation. Hence, the DHOase domain does not appear to contribute directly to CAD oligomerization, though it may still play an indirect role.

Previous studies (28, 29) indicated that many oligomeric enzymes or their subunits can reversibly dissociate and reassociate under certain conditions. In a review by Traut (28), more than 40 dissociating enzymes of metabolic pathways were listed. Moreover, 82% of these enzymes were inactive as dissociated monomers. That work focused on dissociating conditions such as enzyme concentration, ligand concentration, other cellular proteins, pH, and temperature. The importance of divalent cations such as magnesium was not described. Here, although the high concentration of magnesium and the substitutions of ATCase residues are not *in vivo* physiological variables, the concentration of magnesium may still be relevant to the oligomeric state of other enzymes. In our study, high concentrations of magnesium were found to lead to CAD monomers in the altered CADs, whereas low concentrations of magnesium led to various oligomeric forms. This result may explain why the MBP-ATCase experiments previously showed D90A and R269A as trimers and dimers on nondenaturing gel electrophoresis (low magnesium) (9). When the MBP-ATCase mutants were sedimented through glycerol gradients with 25 mM magnesium, they too, behaved as monomers (unpublished data), consistent with the findings here for full-length CAD. Low magnesium concentration does not uniquely restore the CAD ATCase substituted protein to hexamer, raising the possibility that low magnesium concentration leads to some extent to nonspecific aggregation.

Most previous structural studies of CAD focused on the enzyme in the absence of substrates (1, 26). As in the initial glycerol sedimentation study without added substrates, we found that the wild-type CAD was hexameric, but the altered CADs were monomeric. There are no data to support that any ATCase is enzymatically active as a monomer. In fact, genetic data from Schachman's lab (24) indicate that the active site requires interactions of C1 and C2 subunits. The crystallography of *E. coli* ATCase (3) and the comparative modeling of mammalian ATCase (25) all demonstrate that the trimeric forms are prerequisite for ATCase catalysis because the residues from adjacent subunits are involved in constituting the active sites. Thus, the finding of activity in CAD-R269A sedimented in a gradient with 25 mM magnesium was unexpected. This led to the hypothesis that the altered CAD polypeptides formed oligomers when the substrates were present.

PALA is a bisubstrate analogue for the substrates of ATCase. Reports about *E. coli* ATCase (30) indicated that the binding of PALA caused a conformational transition of the enzyme from the T state to the R state. In our conformational study of CAD, PALA was chosen to mimic the activated complex. As shown here, PALA did induce the monomeric CAD-R269A to associate into hexamers. This result and the later experiment with both ATCase substrates demonstrate that they can compensate for a loss of the Asp-90–Arg-269 pairing at the interfaces of the C1 and C2 subunits. These data supported the hypothesis stated above, explaining how protein sedimenting as a monomer in the gradient could be active in the subsequent enzyme assay. The dissociation of the altered CADs can be reversed upon the addition of the transition state analogue or the ATCase substrate carbamoyl phosphate. A similar effect by carbamoyl phosphate was recently reported for the catalytic subunits of the ATCase from *Sulfolobus acidocaldarius* (31).

Like the MBP-ATCase with substitutions, CAD-R269A ATCase activity might be extremely sensitive to temperature. The findings for carbamoyl phosphate discussed above suggest that CAD-R269A ATCase activity in the presence of a high Mg^{2+} concentration and carbamoyl phosphate might be more thermostable than the same enzyme in the presence of only high Mg^{2+}. Preliminary results (J.N.D., Y.Q., and S. R. Maiti, unpublished data) indicate that this prediction is correct.

The present study showed that aspartate did not have any effect on the oligomeric state of the altered CADs. This result means either that aspartate might bind to the enzyme without affecting the oligomeric state or that aspartate cannot bind to the enzyme without the prior binding of carbamoyl phosphate. Previous studies on *E. coli* ATCase (32–36) showed that catalysis followed an ordered mechanism with carbamoyl phosphate binding first and inducing a conformational change that permits aspartate to bind (37). The experiments reported here indicate that the ATCase of CAD may follow a similar ordered mechanism. Our altered CADs may provide a unique tool to reveal the conformational transition caused by carbamoyl phosphate binding to the enzyme, a transition not easily viewed with the wild-type CAD.

Carbamoyl phosphate can break down and release phosphate. It is possible that phosphate rather than the carbamoyl phosphate binds to the enzyme and induces the oligomerization. Previous studies (32) have indicated that phosphate is a competitive inhibitor of ATCase. However, if the concentration of carbamoyl phosphate is high enough, it should replace the binding of phosphate to the enzyme. In our experiment, the saturating concentration of carbamoyl phosphate was used (2.5 mM). Such high concentration of carbamoyl phosphate available makes it unlikely that P_i itself had any significant effect.

Carbamoyl phosphate is an unstable intermediate produced by CPSase that must reach the ATCase domain. It has been suggested that partial metabolic channeling allows the transfer of carbamoyl phosphate to the active site of ATCase without substantial leakage or exposure to the solution (11, 38). Because the CPSase reaction is the rate-limiting step in the pathway, channeling may be essential so that the local concentration of carbamoyl phosphate might be high enough to bind the ATCase efficiently. Glycerol sedimentation of CAD-R269A may provide an approach to show not only that channeling might involve a close encounter of the CPSase and ATCase domains but also that the intermediate carbamoyl phosphate plays a role in holding the ATCase domain in an activated state. Channeling may be meaningful in explaining why the multifunctional CAD has arisen from an ancient gene fusion (39).

We thank Alan J. Simmons for helpful comments on the manuscript. This work was supported through the funding of the National Science Foundation (MCB-98–08562) and the National Institutes of Health (GM47644) and by the core facilities of the Lucille Markey Cancer Center.

1. Coleman, P. F., Suttle, D. P. & Stark, G. R. (1977) *J. Biol. Chem.* **252,** 6379–6385.
2. Evans, D. R. (1986) in *Multidomain Proteins: Structure and Evolution,* eds. Hardie, D. G. & Coggins, J. R. (Elsevier, New York), pp. 283–331.
3. Stevens, R. C., Chook, Y. M., Cho, C. Y., Lipscomb, W. N. & Kantrowitz, E. R. (1991) *Protein Eng.* **4,** 391–408.
4. Simmer, J. P., Kelly, R. E., Scully, J. L., Grayson, D. R., Rinker, A. G., Jr., Bergh, S. T. & Evans, D. R. (1989) *Proc. Natl. Acad. Sci. USA* **86,** 4382–4386.
5. Grayson, D. R. & Evans, D. R. (1983) *J. Biol. Chem.* **258,** 4123–4129.
6. Maley, J. A. & Davidson, J. N. (1988) *Mol. Gen. Genet.* **213,** 278–284.
7. Baker, D. P. & Kantrowitz, E. R. (1993) *Biochemistry* **32,** 10150–10158.
8. Davidson, J. N. & Wales, M. E. (1996) *Paths to Pyrimidines* **4,** 11–17.
9. Qiu, Y. & Davidson, J. N. (1998) *Biochem. J.* **329,** 243–247.
10. Musmanno, L. A., Jamison, R. S., Barnett, R. S., Buford, E. & Davidson, J. N. (1992) *Somatic Cell Mol. Genet.* **18,** 309–318.
11. Guy, H. I. & Evans, D. R. (1994) *J. Biol. Chem.* **269,** 23808–23816.
12. Rees, S., Coote, J., Stables, J., Goodson, S., Harris, S. & Lee, M. G. (1996) *BioTechniques* **1,** 102–104, 106, 108–110.
13. Sambrook, J., Fritsch, E. F. & Maniatis, T. (1989) *Molecular Cloning*: *A Laboratory Manual* (Cold Spring Harbor Lab. Press, Plainview, NY), 2nd Ed.
14. Bradford, M. M. (1976) *Anal. Biochem.* **72,** 248–254.
15. Patterson, D. & Carnright, D. V. (1977) *Somatic Cell Genet.* **3,** 483–495.
16. Shaw, S. M. & Carry, E. A. (1992) *Eur. J. Biochem.* **207,** 957–965.
17. Simmons, A. J., Rawls, J. M., Piškur, J. & Davidson, J. N. (1999) *J. Mol. Biol.* **287,** 277–285.
18. Christopherson, R. I., Matsuura, T. & Jones, M. E. (1978) *Anal. Biochem.* **89,** 225–234.
19. Mally, M. I., Grayson, D. R. & Evans, D. R. (1980) *J. Biol. Chem.* **255,** 11372–11380.
20. Collins, K. D. & Stark, G. R. (1971) *J. Biol. Chem.* **246,** 6599–6605.
21. Swyryd, E. A., Seaver, S. S. & Stark, G. R. (1974) *J. Biol. Chem.* **249,** 6945–6950.
22. Kempe, T. D., Swyryd, E. A., Bruist, M. & Stark, G. R. (1976) *Cell* **9,** 541–550.
23. Banerjei, L. C. & Davidson, J. N. (1997) *Somatic Cell Mol. Genet.* **23,** 37–49.
24. Lahue, R. S. & Schachman, H. K. (1984) *J. Biol. Chem.* **259,** 13906–13913.
25. Scully, J. L. & Evans, D. R. (1991) *Proteins Struct. Funct. Genet.* **9,** 191–206.
26. Lee, L., Kelly, R. E., Pastra-Landis, S. C. & Evans, D. R. (1985) *Proc. Natl. Acad. Sci. USA* **82,** 6802–6806.
27. Carry, E. A. (1995) *Paths to Pyrimidines* **3,** 68–72.
28. Traut, T. W. (1994) *Crit. Rev. Biochem. Mol. Biol.* **29,** 125–163.
29. Traut, T. W. (1988) *Crit. Rev. Biochem.* **23,** 121–169.
30. Ke, H. M., Lipscomb, W. N., Cho, Y. J. & Honzatko, R. B. (1988) *J. Mol. Biol.* **204,** 725–747.
31. Durbecq, V., Thia-Toong, T.-L., Charlier, D., Villeret, V., Roovers, M., Wattiez, R., Legrain, C. & Glansdorff, N. (1999) *Eur. J. Biochem.* **264,** 233–241.
32. Porter, R. W., Modebe, M. O. & Stark, G. R. (1969) *J. Biol. Chem.* **244,** 1846–1859.
33. Schaffer, M. E. & Stark, G. R. (1972) *Biochem. Biophys. Res. Commun.* **46,** 2082–2086.
34. Wedler, F. C. & Gasser, F. J. (1974) *Arch. Biochem. Biophys.* **163,** 57–68.
35. Hsuanyu, Y. & Wedler, F. C. (1987) *Arch. Biochem. Biophys.* **259,** 316–330.
36. Parmentier, L. E., O'Leary, M. H., Schachman, H. K. & Cleland, W. W. (1992) *Biochemistry* **31,** 6570–6576.
37. England, P., Leconte, C., Tauc, P. & Hervé, G. (1994) *Eur. J. Biochem.* **222,** 775–780.
38. Irvine, H. S., Shaw, S. M., Paton, A. & Carry, E. A. (1997) *Eur. J. Biochem.* **247,** 1063–1073.
39. Davidson, J. N., Chen, K. C., Jamison, R. S., Musmanno, L. A. & Kern, C. B. (1993) *BioEssays* **15,** 157–164.